External coupling efficiency in planar organic light-emitting devices

M.-H. Lu[a] and J. C. Sturm
Center for Photonics and Optoelectronic Materials, Department of Electrical Engineering, Princeton University, Princeton, New Jersey 08544

(Received 31 October 2000; accepted for publication 26 January 2001)

The external coupling efficiency in planar organic light-emitting devices is modeled based on a quantum mechanical microvavity theory and measured by examining both the far-field emission pattern and the edge emission of light trapped in the glass substrate. The external coupling efficiency is dependent upon the thickness of the indium–tin–oxide layer and the refractive index of the substrate. The coupling efficiency ranges from ~24% to ~52%, but in general it is much larger than the 18.9% expected from classical ray optics. © *2001 American Institute of Physics.*
[DOI: 10.1063/1.1357207]

There has been enormous interest in organic light-emitting devices (OLEDs) primarily due to their application in flat panel displays. One critical figure of merit for OLEDs is the external coupling efficiency, $\eta_{cp,ext}$, which links the external quantum efficiency (photon/electron), η_{ext}, to the internal quantum efficiency, η_{int}, by the relation $\eta_{ext} = \eta_{cp,ext}\eta_{int}$.

The typical OLED consists of a multilayer sandwich of a planar glass substrate, a layer of indium–tin–oxide (ITO), one or more organic layers, and a reflecting cathode. The light is emitted into three types of modes: the external modes where the light escapes the substrate, the substrate-waveguided modes, and the ITO/organic-waveguided modes (Fig. 1).[1,2] According to classical ray optics theory, the coupling efficiencies of the external, substrate, and ITO/organic modes are 18.9%, 34.2%, and 46.9%, respectively.[1,2] This leads to an unrealistically high estimate for the internal quantum efficiency in some efficient devices.[3,4] In addition, several groups have reported dependence of the far-field emission pattern on the thickness of the organic layer, which is not explained by the classical theory.[5,6] Studies of the directionality and spectrum of the external emission have been carried out using wave optics.[7–11] Most recently, a half-space radiating dipole model was used to describe the external and substrate modes of a polymer OLED.[12] On the other hand, a quantum mechanical (QM) microcavity theory has been shown to accurately predict the emission into all three modes as a function of the OLED layered structure.[6,13] In this letter, we use this model to compute the distribution of light emission among the three modes, and to examine the effects of the thickness of the ITO layer and the index of refraction of the substrate on this distribution. Finally, the modeling results are correlated with experimental measurements.

Since the layers in a typical OLED are much thinner than the emission wavelength, external coupling of light is poorly described by classical ray optics. A quantum mechanical microcavity theory of OLEDs developed by Bulović *et al.* has been used to calculate the distribution of light emission into various modes and to predict the amount of increase in external emission by attaching a lens to the backside of the substrate.[6,13] In this formulation, the exciton is modeled as a radiating dipole whose decay rate is given by Fermi's golden rule. The electric fields for transverse electric (TE) and transverse magnetic (TM) modes are calculated using standard microcavity theory[14] assuming the cathode is a perfect reflector. In our devices (Fig. 1), the excitons were assumed to be created at the electron transporter/hole transporter [tris-(8-hydroxyquinoline)aluminum (Alq_3)/poly-(*N*-vinylcarbazole) (PVK) in our devices] interface and to diffuse into the Alq_3 with a characteristic decay length of 20 nm.[15] Nonradiative energy transfer to the cathode was taken into account by using the results in Ref. 13.

First, we calculate the distribution of the emitted light in our bilayer OLEDs with the following structure: soda lime glass/100 nm ITO/40 nm PVK/80 nm Alq_3. Figure 2 illustrates the radiation pattern near the peak of the Alq_3 spectrum ($\lambda = 524$ nm), where the QM microcavity results are in stark contrast to the isotropic radiation of the classical model. The external and substrate modes are a continuum since the distance of observation and the thickness of the glass substrate are much greater than the wavelength in question. The combined ITO/organic layer thickness is on the order of a half wavelength, so the modes there, if they exist, are discrete. In this particular example, no ITO/organic mode exists for either TE or TM radiation. In general, the energy in these ITO/organic modes may be significant, but still less

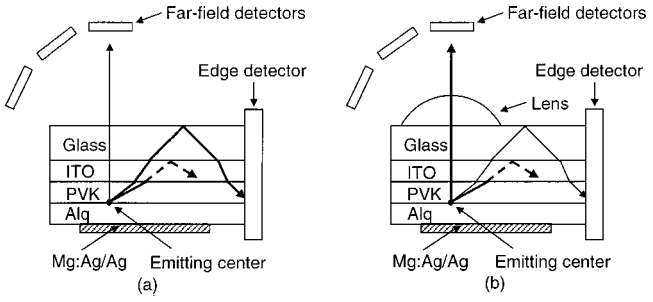

FIG. 1. Schematic diagram of OLEDs on soda lime glass substrates and the measurement setup. (a) In the planar OLED, a large portion of the light is trapped in the substrate and enters the edge detector. (b) After attaching a lens to the backside, some light trapped in the substrate is emitted externally. In both cases, the ITO/organic modes are heavily attenuated by the ITO layer.

[a]Electronic mail: minhaolu@ee.princeton.edu

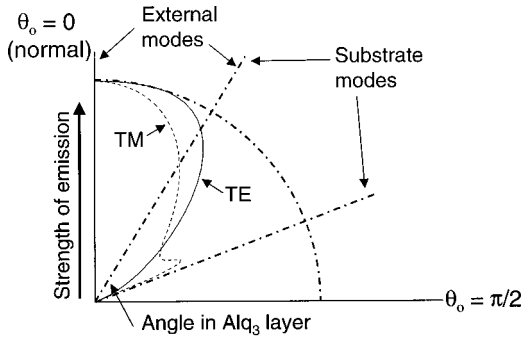

FIG. 2. Calculated polar plot of modal strength vs mode angle in Alq_3 for at $\lambda = 524$ nm (OLED structure: standard glass/100 nm ITO/40 nm PVK/80 nm Alq_3/Mg:Ag. The exciton is at the PVK/Alq_3 interface). Solid line: TE mode; dashed line: TM mode; dash-dotted arc: ray optics model. The external and substrate modes are a continuum. There are no ITO/organic modes in this case. The cutoff wavelength is ~452 nm for TE modes and ~440 nm for TM modes.

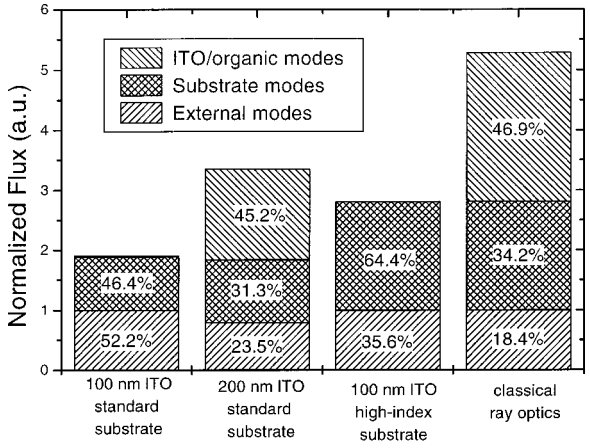

FIG. 4. Calculated distribution of emission into external, substrate, and ITO/organic modes for various OLED structures (glass substrate/ITO/40 nm PVK/80 nm Alq_3/Mg:Ag). The fluxes into the external modes of the sample with 80 nm Alq_3 on standard substrates and the classical model are normalized to 1.

than what ray optics would predict. The reduced emission at large angles in the substrate and ITO/organic modes constitutes the main difference between the QM and the classical models.

The flux emitted into each of the three categories of modes is obtained by integrating or summing over the appropriate wave vectors, weighted by the exciton distribution profile and the photoluminescence (PL) spectrum of Alq_3. Figure 3 shows the calculated far-field intensity pattern compared with the experimental data. Unlike inside the Alq_3 (see Fig. 2), the TM modes at large far-field angles have slightly higher intensity than the TE modes due to a larger glass to air transmission coefficient for TM modes at large angles. This effect is visible in both the modeling and the data.

The thickness of the ITO layer affects the modal distribution in two ways. It alters the ITO/organic modes by changing the combined thickness of the ITO/organic layer, and the external and substrate modes through interference effects. It is possible to have an ITO layer so thin that no mode exists for most of the visible spectrum. The distribution of light emission is calculated for OLEDs with 100 and 200 nm thick ITO layers (Fig. 4). The emission into the ITO/organic modes in the OLED with the thinner ITO layer is drastically suppressed, since the cutoff wavelength is only slightly above the low end of the visible spectrum. On the other hand, the cutoff is above the peak emission wavelength of Alq_3 in the OLED with the 200 nm ITO layer, resulting in much stronger ITO/organic modes. The absolute value of the emission in the external and substrate modes is moderately affected by the interference effects, but not enough to prevent the proportion of external emission from increasing with decreasing ITO layer thickness. According to our calculations, as much as ~52% of the light could be emitted externally in the planar device with 100 nm ITO.

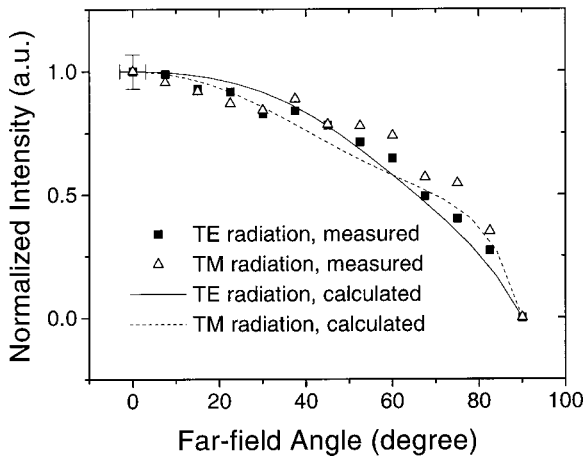

FIG. 3. Measured and calculated far-field emission pattern (OLED structure: standard glass/100 nm ITO/40 nm PVK/80 nm Alq_3/Mg:Ag). Typical error bars are shown on the first data point of TE modes.

On standard soda lime glass substrates, the confinement of the ITO/organic modes hinges on the fact that the glass substrate has a lower index of refraction than that of the emitting layer, so that some light is trapped by total internal refraction (TIR) at the ITO/glass interface. A high-index-of-refraction substrate completely eliminates the TIR, subsequently converting the ITO/organic modes into substrate modes.[16,17] This effect is illustrated in Fig. 4 where the distribution is again calculated for identical devices on standard and high-index glass substrates. There is no change in the external emission because it is not dependent upon the index of the intervening layers. But the total emission is different because all modes in the OLED on high-index substrates are continuum modes, whereas the ITO/organic modes in OLEDs on standard substrates are discretized and suppressed. In the short wavelength length limit, the total emission would have been the same. This extra emission into the substrate modes is most relevant to backside patterning techniques where the substrate modes are made to emit externally.[16,17]

Bilayer OLEDs were fabricated on 0.5 mm thick soda lime ($n_{glass1} = 1.51$) glass and high-index glass (Schott SFL57, $n_{glass2} = 1.85$) substrates. ITO ($n_{ITO} = 2.0$) layers, 100 or 200 nm in thickness, were deposited by rf magnetron sputtering with no intentional heating. The sheet resistance of the 100 nm thick ITO was approximately 100 Ω/sq, and the transmission was ~80% in the visible. The hole transport layer in all devices was a 40 nm layer of PVK($n_{PVK} = 1.67$), deposited by spin coating after the ITO surface was treated by an O_2 plasma.[13] The electron transport and emit-

TABLE I. Measured values of $\eta_{cp,ext}/\eta_{cp,sub}$ compared with the calculations based on the QM microcavity model for different device structures. The thicknesses of the PVK and Alq_3 layers are 40 and 80 nm, respectively.

Sample	Measured value	Model value
Soda lime glass/100 nm ITO/PVK/Alq_3/Mg:Ag/Ag	1.30±0.20	1.12
Soda lime glass/200 nm ITO/PVK/Alq_3/Mg:Ag/Ag	0.51±0.08	0.75
High-index glass/100 nm ITO/PVK/Alq_3/Mg:Ag/Ag	0.41±0.06	0.56

ting layer in all devices were $Alq_3(n_{Alq}=1.71)$, deposited by vacuum sublimation. The cathodes were 30–50 nm of Mg:Ag (10:1) followed by a Ag cap evaporated through a shadow mask with 0.5 mm diam holes. The electroluminescence (EL) spectrum showed that light emission was exclusively from the Alq_3 layer. All lenses used for effective substrate shaping have a radius of curvature of 2.0 mm and a height of 1.5 mm, placing the OLED exactly at the center of the curvature. They were made from the same material as the substrates, and were attached with index-matching oil.

Direct measurement of the substrate and ITO/organic waveguided light is difficult; therefore, we devised a method that indirectly measures the ratio of light emission into the external modes over that into the substrate modes, i.e., $\eta_{cp,ext}/\eta_{cp,sub}$. A portion of substrate waveguided light can be made to emit externally by attaching a lens to the backside of the substrate.[2,6,18] Due to the thickness of the substrate, it was assumed that attaching the lens negligibly affected the behavior of the OLED. Since the ITO/organic modes were heavily attenuated by absorption in the ITO layer, we assumed that the edge emission was exclusively from the substrate modes. It follows that

$$F_{ext}+F_{sub}=F'_{ext}+F'_{sub}=r_1F_{ext}+r_2F_{sub},$$

$$\frac{\eta_{cp,ext}}{\eta_{cp,sub}}=\frac{F_{ext}}{F_{sub}}=\frac{1-r_2}{r_1-1},$$

where F_{ext} and F_{sub} are the fluxes in the external and substrate modes in a planar sample, and the primed symbols are the fluxes after lens attachment. r_1 and r_2 are defined as F'_{ext}/F_{ext} and F'_{sub}/F_{sub}, respectively.

The measured ratios of $\eta_{cp,ext}/\eta_{cp,sub}$ for various devices are summarized in Table I. There was reasonable agreement between the measured and calculated values despite the simplicity of our assumptions such as the absence of mode-mixing scattering. The data confirmed the reduction of emission into the external modes relative to the substrate modes as the ITO thickness was increased and when high-index substrates were used.

A QM microcavity model was used to calculate the detailed distribution of light emission in planar OLEDs. The emission into the external modes were found to be as high as ~52%, much higher than the 18.9% predicted by ray optics. This suggests that the high external quantum efficiency in some efficient devices does not invalidate our basic assumptions about spin statistics in Alq_3.[3,4,19] Experimental measurement of the ratio, $\eta_{cp,ext}/\eta_{cp,sub}$, qualitatively agrees with the model. The main difference between the classical and QM models arises from the relative suppression of modes at large angles from the normal by the microcavity effect.

This work was supported by the New Jersey Commission in Science and Technology (Grant No. 082-2042-007-6130) and the NSF (Grant No. ECS 96-12281).

[1] N. C. Greenham, R. H. Friend, and D. D. C. Bradley, Adv. Mater. **6**, 491 (1994).
[2] C. F. Madigan, M.-H. Lu, and J. C. Sturm, Appl. Phys. Lett. **76**, 1650 (2000).
[3] T. Tsutsui, MRS Bull. **22**, 39 (1997).
[4] J. Kido and Y. Iizumi, Appl. Phys. Lett. **73**, 2721 (1998).
[5] T. Tsutsui, M.-J. Yang, M. Yahiro, K. Nakamura, T. Wantanabe, T. Tsuji, Y. Fukuda, T. Wakimoto, and S. Miyaguchi, Jpn. J. Appl. Phys., Part 2 **38**, L1502 (1999).
[6] M.-H. Lu, C. F. Madigan, and J. C. Sturm, Mater. Res. Soc. Symp. Proc. **621**, Q3.7 (2000).
[7] S. Saito, T. Tsutsui, M. Erra, N. Takada, C. Adachi, Y. Hamada, and T. Wakimoto, Proc. SPIE **1910**, 212 (1993).
[8] V. Cirmova and D. Neher, J. Appl. Phys. **79**, 3299 (1996).
[9] D. G. Lidzey, M. A. Pate, D. M. Whittaker, D. D. C. Bradley, M. S. Weaver, A. A. Fisher, and M. S. Skolnick, Chem. Phys. Lett. **263**, 655 (1996).
[10] J. Gruner, F. Cacialli, and R. H. Friend, J. Appl. Phys. **80**, 207 (1996).
[11] H. F. Wittman, J. Gruner, R. H. Friend, G. W. C. Spencer, S. C. Moratti, and A. B. Holmes, Adv. Mater. **7**, 541 (1995).
[12] J.-S. Kim, P. K. H. Ho, N. C. Greenham, and R. H. Friend, J. Appl. Phys. **88**, 1073 (2000).
[13] V. Bulović, V. B. Khalfin, G. Gu, P. E. Burrows, D. Z. Garbuzov, and S. R. Forrest, Phys. Rev. B **58**, 3730 (1998).
[14] E. Hecht, *Optics*, 3rd ed. (Addison–Wesley, Reading, MA, 1998).
[15] C. W. Tang, S. A. VanSlyke, and C. H. Chen, J. Appl. Phys. **65**, 3610 (1989).
[16] T. Yamasaki, K. Sumioka, and T. Tsutsui, Appl. Phys. Lett. **76**, 1243 (2000).
[17] M.-H. Lu, C. F. Madigan, and J. C. Sturm, Tech. Dig. Int. Electron Devices Meet. 607 (2000).
[18] C.-C. Wu, C.-I. Wu, J. C. Sturm, and A. Khan, Appl. Phys. Lett. **70**, 1348 (1997).
[19] M. A. Baldo, D. F. O'Brien, M. E. Thompson, and S. R. Forrest, Phys. Rev. B **60**, 14422 (1999).